

Bounds on supersymmetric effective operators from heavy diphoton searches

D. M. Ghilencea^{a, b} and Hyun Min Lee^c

^a Theory Division, CERN, 1211 Geneva 23, Switzerland

^b Theoretical Physics Department, National Institute of Physics
and Nuclear Engineering (IFIN-HH) Bucharest 077125, Romania

^c Department of Physics, Chung-Ang University, 06974 Seoul, Korea.

Abstract

We identify the bounds on supersymmetric effective operators beyond MSSM, from heavy diphoton resonance (X) negative searches at the LHC, where X is identified with the neutral CP-even (odd) H (A) or both (mass degenerate). While minimal supersymmetric models (MSSM, etc) comply with the data, a leading effective operator of $d = 6$ can contribute significantly to diphoton production $\sigma \sim 1$ fb, well above its MSSM value and in conflict with recent data. Both the $b\bar{b}$ and gg production mechanisms of H and A can contribute comparably to this. We examine the dependence of the diphoton cross section σ on the values of m_X , Λ and $\tan\beta$, under the experimental constraints from the SM-like higgs couplings hgg and $h\gamma\gamma$ (due to mixing) and from the $b\bar{b}$ and $t\bar{t}$ searches. These give Λ larger than ~ 5 TeV for m_X in the range $0.5 - 1$ TeV. We show how to generate the $d = 6$ effective operator from microscopic (renormalizable) models. This demands the presence of vector-like states beyond the MSSM spectrum (and eventually but not necessarily a gauge singlet), of mass near Λ and thus outside the LHC reach.

1 Motivation

Current searches for new physics at the LHC bring increasingly strong constraints on the parameter space of supersymmetric models. Consider for example a final diphoton state at the LHC. Then at the parton level, the exchange of a state X of spin J , mass m_X and width Γ_X has a cross section

$$\sigma(pp \rightarrow X \rightarrow \gamma\gamma) = \frac{2J+1}{s m_X} \left[\sum_p C_{p\bar{p}} \Gamma(X \rightarrow p\bar{p}) \right] \frac{\Gamma(X \rightarrow \gamma\gamma)}{\Gamma_X} \quad (1)$$

where the sum is over partons $p = \{g, b, c, s, u, d, \gamma\}$. $C_{p\bar{p}}$ are partonic integrals coefficients evaluated at m_X . LHC searches for a heavy diphoton resonance (X) can impact on model building beyond the Standard Model (SM), in particular on supersymmetric models.

Much interest was raised by the initial claim by ATLAS and CMS Collaborations at $\sqrt{s}=13$ TeV of a possible diphoton final state of $m_X = 750$ GeV with an excess relative to the SM [1] (also [2, 3]), with $\sigma(pp \rightarrow \gamma\gamma)_{\text{ATLAS}} = 10 \pm 3 \text{ fb}$ and $\sigma(pp \rightarrow \gamma\gamma)_{\text{CMS}} = 6 \pm 3 \text{ fb}$. Further, the analysis of additional data invalidated this claim [4]. This is actually welcome for minimal supersymmetric models (MSSM, etc) where it is not possible to have a heavy resonance X with such significant σ [5], except if¹: a): one is fine-tuning the parameters [11] with X the CP even/odd heavy higgs $X = H, A$, or b): considers the rather special case of low, TeV-scale supersymmetry breaking with X a sgoldstino [12], see also [13, 14, 15].

However, we show that effective operators beyond the MSSM (minimal) higgs sector can contribute dramatically to the diphoton production (giving $\sigma \sim \text{few fb}$) not seen in the data [4]. The resonance X is the CP-odd/even neutral MSSM higgs A or H or *both* (mass degenerate). This result is due to enhanced couplings of the higgs sector to SM gauge bosons, induced by the following *unique, leading* operator of dimension $d=6$

$$(1/\Lambda^2) \int d^2\theta (H_1.H_2) \text{Tr} W^\alpha W_\alpha + \text{h.c.}, \quad (2)$$

where W_α is the supersymmetric field strength of the SM sub-groups $U(1)_Y, SU(2)_L, SU(3)$.

Depending on Λ , operator (2) can bring a large correction to the diphoton production in conflict with the latest data, with impact on H, A searches. Motivated by this, we study the constraints on this operator and examine the dependence of the diphoton cross section σ on the values of m_X, Λ and $\tan\beta$, while including both the $b\bar{b}$ and gg production mechanisms of $X = A, H$. The experimental constraints on the SM-like higgs (h) couplings hgg and $h\gamma\gamma$ and on the $b\bar{b}$ ($t\bar{t}$) cross section (that receive corrections from (2)), are also applied, with impact on the allowed m_X, Λ and $\tan\beta$. For a given $\sigma \sim 0.1 - 1 \text{ fb}$, we illustrate these constraints for $m_{H,A}$ in the range $0.5 - 1 \text{ TeV}$ (in particular for the absent “resonance” at 750 GeV). We then show how operator (2) is generated in a renormalizable model beyond MSSM; an extra $d=5$ operator may also be generated (in some cases) and does not directly affect the diphoton production but may improve naturalness [16].

¹ Many non-supersymmetric explanations were reported for this 750 GeV “resonance”, see [6] for a long list of references. X was a scalar singlet with couplings to new TeV states that mediate (at loop level) its production by gg fusion and its decay to $\gamma\gamma$ [7, 8]. For a non-supersymmetric effective study see [9, 10].

In section 2 we study the new couplings induced in the MSSM higgs sector by the $d=6$ effective operator and its effect on the diphoton production. Section 3 shows how these operators are generated in a renormalizable model. Our conclusions are found in Section 4.

2 Effective operators and diphoton resonance

We consider the MSSM model extended by (supersymmetric) effective operators in the higgs sector and study the diphoton production cross section σ due to a possible resonance X identified with H and/or A . We compute the corrections to the couplings of H , A and h , and the branching ratios of H , A . We then illustrate the correlations between the values of Λ , m_X , $\tan\beta$ and σ , consistent with the constraints from Higgs signals/decays.

2.1 New couplings from effective operators beyond MSSM

From all effective operators of dimensions $d = 5$ and $d = 6$ [16, 17, 18] beyond the MSSM higgs sector, we find only one leading operator that can contribute to a diphoton resonance

$$\mathcal{L}_j = \frac{c_j}{2\Lambda^2 g_j^2 \kappa_j} \int d^2\theta (H_2 \cdot H_1) \text{Tr} (W^\alpha W_\alpha)_j + \text{h.c.} \quad (3)$$

which has dimension $d = 6$. Here $j = 1, 2, 3$ labels the $U(1)_Y$, $SU(2)_L$, $SU(3)$ gauge groups of gauge couplings g_j , so we actually have three operators, with coefficients² $c_j = \mathcal{O}(1)$ and Λ a free parameter. κ_j is a constant that cancels the trace factor. $(W^\alpha)_j$ is the field strength of a vector superfield V_j . The relevant part is³

$$\mathcal{L}_j \supset \frac{c_j}{\Lambda^2} \left[(h_1 \cdot h_2) (F_j^{a\mu\nu} F_{j\mu\nu}^a + i F_{j\mu\nu}^a \tilde{F}_j^{a\mu\nu}) + \text{h.c.} \right] \quad (4)$$

with $\tilde{F}^{\mu\nu} = (1/2) \epsilon^{\mu\nu\rho\sigma} F_{\rho\sigma}$. With real c_j one has, in a standard notation

$$\begin{aligned} \mathcal{L}_1 + \mathcal{L}_2 \supset & \frac{v}{\Lambda^2} \left[(c_{\gamma\gamma} h + b_{\gamma\gamma} H) F_{\mu\nu} F^{\mu\nu} + (c_{\gamma z} h + b_{\gamma z} H) F_{\mu\nu} Z^{\mu\nu} \right. \\ & + (c_{zz} h + b_{zz} H) Z_{\mu\nu} Z^{\mu\nu} + (c_{ww} h + b_{ww} H) W_{\mu\nu}^+ W^{-\mu\nu} \\ & \left. + a_{\gamma\gamma} A F_{\mu\nu} \tilde{F}^{\mu\nu} + a_{zz} A Z_{\mu\nu} \tilde{Z}^{\mu\nu} + a_{\gamma z} A F_{\mu\nu} \tilde{Z}^{\mu\nu} + a_{ww} A W_{\mu\nu}^+ \tilde{W}^{-\mu\nu} \right] \quad (5) \end{aligned}$$

where $F_{\mu\nu}$ is the photon field strength, H (A) are the CP-even (odd) neutral higgses and

$$\begin{aligned} a_{\gamma\gamma} &= -(c_1 c_w^2 + c_2 s_w^2), & a_{zz} &= -(c_1 s_w^2 + c_2 c_w^2), & a_{\gamma z} &= -(c_2 - c_1) s_{2w}, & a_{ww} &= -2c_2 \\ b_{\gamma\gamma} &= -a_{\gamma\gamma} s_{\alpha\beta}, & b_{zz} &= -a_{zz} s_{\alpha\beta}, & b_{\gamma z} &= -a_{\gamma z} s_{\alpha\beta}, & b_{ww} &= -a_{ww} s_{\alpha\beta} \\ c_{\gamma\gamma} &= -a_{\gamma\gamma} c_{\alpha\beta}, & c_{zz} &= -a_{zz} c_{\alpha\beta}, & c_{\gamma z} &= -a_{\gamma z} c_{\alpha\beta}, & c_{ww} &= -a_{ww} c_{\alpha\beta} \quad (6) \end{aligned}$$

²The coefficients $c_j = \mathcal{O}(1)$, $j = 1, 2, 3$ enable us later to turn on/off any of operators $\mathcal{L}_{1,2,3}$.

³Notation used: $h_1 \cdot h_2 = h_1^0 h_2^0 - h_1^- h_2^+$; also $\text{Re } h_1^0 = H \cos \alpha - h \sin \alpha$, $\text{Re } h_2^0 = H \sin \alpha + h \cos \alpha$.

with the notations: $c_{\alpha\beta} = \cos(\alpha + \beta)$, $s_{\alpha\beta} = \sin(\alpha + \beta)$, $c_{2\beta} = \cos(2\beta)$, $c_w = \cos\theta_w$, $s_w = \sin\theta_w$, $s_{2w} = \sin 2\theta_w$. Let us also consider the effect of the gluon operator⁴

$$\mathcal{L}_3 \supset \frac{v}{\Lambda^2} \left[c_{gg} h \text{Tr} G_{\mu\nu} G^{\mu\nu} + b_{gg} H \text{Tr} G_{\mu\nu} G^{\mu\nu} + a_{gg} A \text{Tr} G_{\mu\nu} \tilde{G}^{\mu\nu} \right] \quad (7)$$

where

$$a_{gg} = -c_3, \quad b_{gg} = c_3 s_{\alpha\beta}, \quad c_{gg} = c_3 c_{\alpha\beta}. \quad (8)$$

The Lagrangian of the MSSM corrected with $\mathcal{L}_{1,2,3}$ induces the following couplings

$$\begin{aligned} \mathcal{L} = & \frac{1}{v} \left[(\hat{c}_{\gamma\gamma} h + \hat{b}_{\gamma\gamma} H) F_{\mu\nu} F^{\mu\nu} + (\hat{c}_{\gamma z} h + \hat{b}_{\gamma z} H) F_{\mu\nu} Z^{\mu\nu} + (\hat{c}_{zz} h + \hat{b}_{zz} H) Z_{\mu\nu} Z^{\mu\nu} \right. \\ & + (\hat{c}_{ww} h + \hat{b}_{ww} H) W_{\mu\nu}^+ W^{-\mu\nu} + \hat{a}_{\gamma\gamma} A F_{\mu\nu} \tilde{F}^{\mu\nu} + \hat{a}_{zz} A Z_{\mu\nu} \tilde{Z}^{\mu\nu} + \hat{a}_{\gamma z} A F_{\mu\nu} \tilde{Z}^{\mu\nu} \\ & \left. + \hat{a}_{ww} A W^{+\mu\nu} \tilde{W}_{\mu\nu}^- + (\hat{c}_{gg} h + \hat{b}_{gg} H) \text{Tr} G_{\mu\nu} G^{\mu\nu} + \hat{a}_{gg} A \text{Tr} G_{\mu\nu} \tilde{G}^{\mu\nu} \right]. \quad (9) \end{aligned}$$

The coefficients \hat{a} , \hat{b} and \hat{c} above are related to their counterparts without a hat:

$$\begin{aligned} \hat{\tau}_{\gamma\gamma} &= \frac{\alpha_{\text{em}}}{8\pi} \tau_{\gamma\gamma}^{\text{loop}} + \frac{v^2}{\Lambda^2} \tau_{\gamma\gamma}, & \hat{\tau}_{zz} &= \frac{\alpha_{\text{em}}}{8\pi} \tau_{zz}^{\text{loop}} + \frac{v^2}{\Lambda^2} \tau_{zz}, \\ \hat{\tau}_{gg} &= \frac{\alpha_3}{12\pi} \tau_{gg}^{\text{loop}} + \frac{v^2}{\Lambda^2} \tau_{gg}, & \hat{\tau}_{ww} &= \frac{\alpha_{\text{em}}}{8\pi} \tau_{ww}^{\text{loop}} + \frac{v^2}{\Lambda^2} \tau_{ww}, \\ \hat{\tau}_{\gamma z} &= \frac{\alpha_{\text{em}}}{8\pi s_w} \tau_{\gamma z}^{\text{loop}} + \frac{v^2}{\Lambda^2} \tau_{\gamma z}, & \text{where } \tau &= a, b, c. \end{aligned} \quad (10)$$

The coefficients multiplying v^2/Λ^2 are those of eqs.(6), (8). Further, the coefficients a^{loop} , b^{loop} , c^{loop} are loop-induced, due to the MSSM (in the absence of the effective operators). They bring a very small branching ratio to photons [5] relative to v^2/Λ^2 terms and we present them in Appendix A in the decoupling limit ($\alpha \rightarrow \beta - \pi/2$) in which we work in this paper. We show that their corrected version \hat{a} , \hat{b} , \hat{c} of eqs.(9), (10) can bring a heavy diphoton resonance of large $\sigma \sim 1$ fb, in our model defined by MSSM extended by eq.(3), in possible conflict with the latest data.

2.2 Decay branching ratios of A and H

To discuss the diphoton production we first analyze the impact of the corrections in eq.(9), (10) on the decay rates of the heavy neutral CP-even (odd) Higgs H (A), respectively. The decay rate of H is $\Gamma_H = \sum_i \Gamma(H \rightarrow i)$, where

$$\begin{aligned} \Gamma(H \rightarrow t\bar{t}) &= \frac{N_c m_t^2}{8\pi v^2} \cot^2 \beta m_H (1 - 4x_t)^{3/2}, \\ \Gamma(H \rightarrow b\bar{b}) &= \frac{N_c m_b^2}{8\pi v^2} \tan^2 \beta m_H (1 - 4x_b)^{3/2}, \quad x_i \equiv m_i^2/m_H^2 \end{aligned} \quad (11)$$

⁴If c_3 has an imaginary part, one also has $\mathcal{L}_3 \supset v/\Lambda^2 [\tilde{a}_{gg} A^0 \text{Tr} G^2 + \tilde{b}_{gg} H \text{Tr} G \tilde{G} + \tilde{c}_{gg} h \text{Tr} G^2]$ with $\tilde{a}_{gg} = -\text{Im}[c_3]$, $\tilde{b}_{gg} = -\text{Im}[c_3] \sin(\alpha + \beta)$, $\tilde{c}_{gg} = -\text{Im}[c_3] \cos(\alpha + \beta)$.

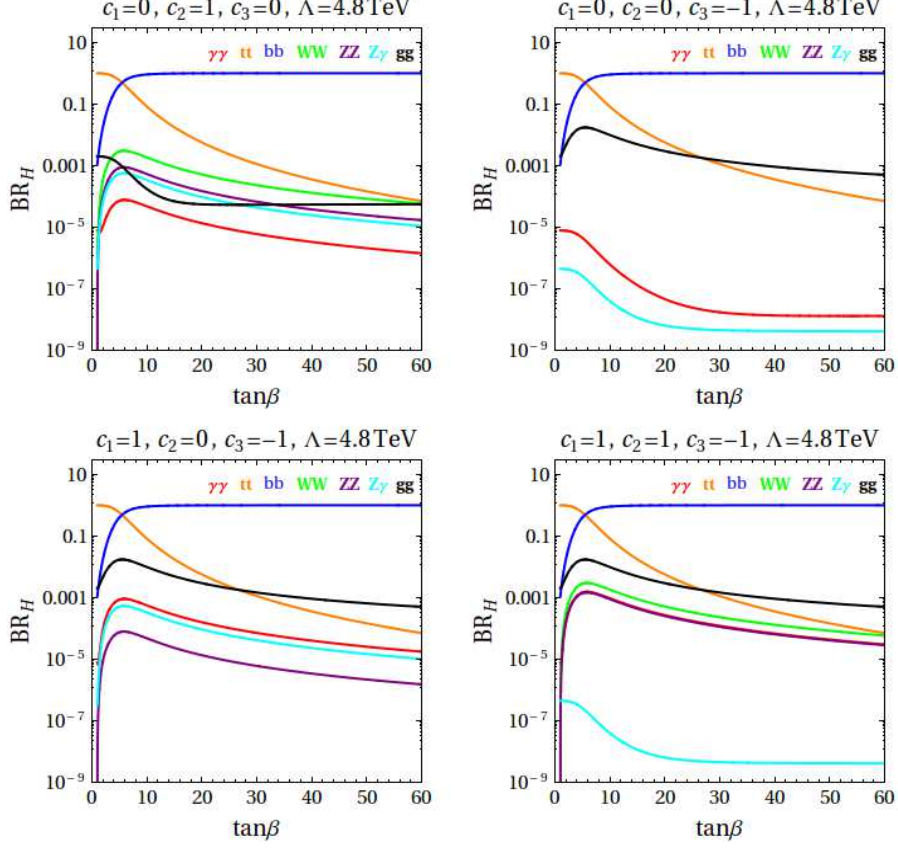


Figure 1: Branching ratios of $H \rightarrow \gamma\gamma, t\bar{t}, b\bar{b}, WW, ZZ, Z\gamma$ and gg , for different $c_{1,2,3}$ and $\tan\beta$. The case $c_1 = 1, c_2 = c_3 = 0$ (not shown) is similar to $c_1 = 0, c_2 = 1, c_3 = 0$ (without WW). The branching ratios for A into the same final states are similar to those above, for the same parameters. Compared to individual $\mathcal{L}_{1,2,3}$, a combination $\mathcal{L}_1 + \mathcal{L}_3$ or $\mathcal{L}_1 + \mathcal{L}_2 + \mathcal{L}_3$ brings the largest branching ratio of H (A) to $\gamma\gamma$, for appropriate relative signs of $c_j, j = 1, 2, 3$.

valid in the decoupling limit and

$$\begin{aligned}
\Gamma(H \rightarrow \gamma\gamma) &= \frac{1}{4\pi} \left(\frac{\hat{b}_{\gamma\gamma}}{v} \right)^2 m_H^3 \\
\Gamma(H \rightarrow \gamma Z) &= \frac{1}{8\pi} \left(\frac{\hat{b}_{\gamma Z}}{v} \right)^2 m_H^3 (1 - x_Z)^3 \\
\Gamma(H \rightarrow gg) &= \frac{2}{\pi} \left(\frac{\hat{b}_{gg}}{v} \right)^2 m_H^3 \\
\Gamma(H \rightarrow WW) &= \frac{1}{8\pi} \left(\frac{\hat{b}_{ww}}{v} \right)^2 m_H^3 (1 - 4x_W + 6x_W^2)(1 - 4x_W)^{1/2}, \\
\Gamma(H \rightarrow ZZ) &= \frac{1}{4\pi} \left(\frac{\hat{b}_{zz}}{v} \right)^2 m_H^3 (1 - 4x_Z + 6x_Z^2)(1 - 4x_Z)^{1/2}.
\end{aligned} \tag{12}$$

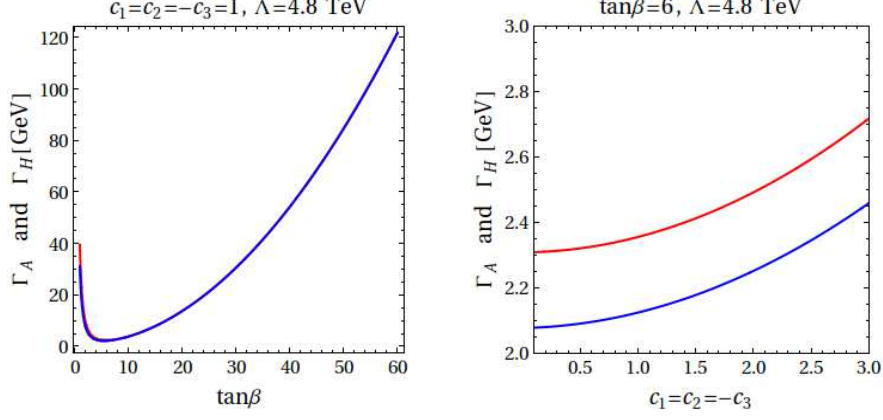


Figure 2: Total decay widths of heavy Higgs fields Γ_H (blue) and Γ_A (red), for $m_{A,H} = 750$ GeV. These plots remain similar for other c_1, c_2, c_3 used later. A narrow width region $\Gamma_X \leq 5$ GeV corresponds to low $2 \leq \tan\beta \leq 12$ while for larger $\tan\beta$ one has a large width regime.

The decay rate of the heavy neutral CP-odd Higgs A is $\Gamma_A = \sum_i \Gamma(A \rightarrow i)$, with

$$\begin{aligned}
\Gamma(A \rightarrow t\bar{t}) &= \frac{N_c m_t^2}{8\pi v^2} \cot^2 \beta m_A (1 - 4\bar{x}_t)^{1/2}, \\
\Gamma(A \rightarrow b\bar{b}) &= \frac{N_c m_b^2}{8\pi v^2} \tan^2 \beta m_A (1 - 4\bar{x}_b)^{1/2}, \\
\Gamma(A \rightarrow \gamma\gamma) &= \frac{1}{4\pi} \left(\frac{\hat{a}_{\gamma\gamma}}{v} \right)^2 m_A^3, \\
\Gamma(A \rightarrow \gamma Z) &= \frac{1}{8\pi} \left(\frac{\hat{a}_{\gamma z}}{v} \right)^2 m_A^3 (1 - \bar{x}_Z)^3, \\
\Gamma(A \rightarrow gg) &= \frac{2}{\pi} \left(\frac{\hat{a}_{gg}}{v} \right)^2 m_A^3, \\
\Gamma(A \rightarrow WW) &= \frac{1}{8\pi} \left(\frac{\hat{a}_{ww}}{v} \right)^2 m_A^3 (1 - 4\bar{x}_W)^{3/2}, \\
\Gamma(A \rightarrow ZZ) &= \frac{1}{4\pi} \left(\frac{\hat{a}_{zz}}{v} \right)^2 m_A^3 (1 - 4\bar{x}_Z)^{3/2}, \quad \bar{x}_i \equiv m_i^2/m_A^2. \quad (13)
\end{aligned}$$

In figure 1 the branching ratios of H decays are presented as functions of $\tan\beta$, for different $c_{1,2,3}$. The dominant decays modes are into $t\bar{t}$ at low $\tan\beta < 6$ and $b\bar{b}$ at large $\tan\beta$ while near $\tan\beta \sim 6$ or so, they are comparable. The remaining decay modes have smaller, often comparable rates. For A , one has nearly identical plots. Compared to individual $\mathcal{L}_{1,2,3}$, a combination $\mathcal{L}_1 + \mathcal{L}_3$ or $\mathcal{L}_1 + \mathcal{L}_2 + \mathcal{L}_3$ brings the largest branching ratio of H (A) to $\gamma\gamma$, for suitable relative signs of $c_{1,2,3}$ (shown). As an illustration, we used $m_X = 750$ GeV ($X = H, A$) but these plots are similar for $500 \leq m_X \leq 1000$ GeV. The total $\Gamma_{H,A}$ is shown in figure 2. $\tan\beta$ controls the width of the resonance X ($X = A$ or H). At low $2 \leq \tan\beta \leq 12$, $\Gamma_X \leq 5$ GeV and one has the limit of narrow width ($\Gamma_X/m_X \ll 1$). Figure 2 remains similar for other $c_{1,2,3} \sim \mathcal{O}(1)$, of different signs, or if c_1 or c_2 vanish.

2.3 Diphoton searches at large $m_{H,A}$

Assuming a resonance $X = H, A$, we include the dominant gg and $b\bar{b}$ production channels and consider the contributions of A and H to a diphoton final state. From eq.(1)

$$\begin{aligned} \sigma(pp \rightarrow \underbrace{H, A}_X \rightarrow \gamma\gamma) &= \frac{1}{sm_H} (K_{gg} C_{gg} \Gamma(H \rightarrow gg) + K_{b\bar{b}} C_{b\bar{b}} \Gamma(H \rightarrow b\bar{b})) \text{Br}(H \rightarrow \gamma\gamma) \\ &+ \frac{1}{sm_A} (K_{gg} C_{gg} \Gamma(A \rightarrow gg) + K_{b\bar{b}} C_{b\bar{b}} \Gamma(A \rightarrow b\bar{b})) \text{Br}(A \rightarrow \gamma\gamma) \end{aligned} \quad (14)$$

where $K_{gg}, K_{b\bar{b}}$ are K-factors, given by $K_{gg} = 1.5, K_{b\bar{b}} = 1.2$, and $C_{gg}, C_{b\bar{b}}$ are parton luminosities. Their values depend on the mass of the resonance, as shown in figure 3, that we generated with the CTEQ5 package [19].

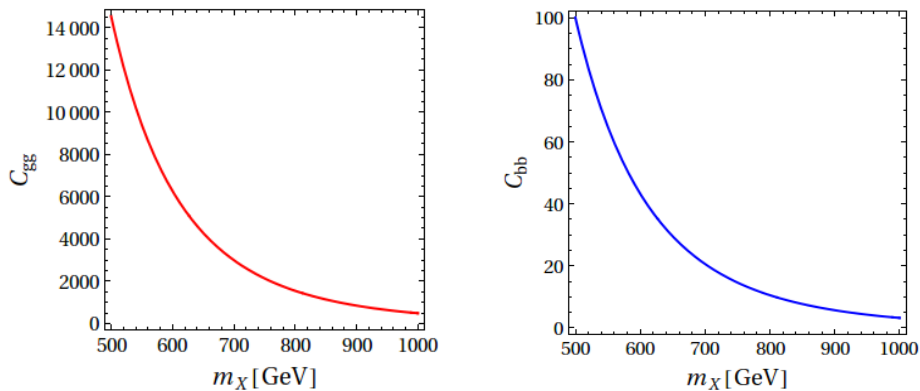


Figure 3: The dependence of partonic integrals coefficients C_{gg} and $C_{b\bar{b}}$ at $\sqrt{s} = 13$ TeV on m_X [19]. In the model considered here $X = H, A$. For example, for $m_X = 750$ GeV one has $C_{gg} = 2131$, $C_{b\bar{b}} = 14.6$; also $C_{\gamma\gamma} \approx 54$, $C_{u\bar{u}} \approx 1054$, $C_{d\bar{d}} \approx 627$, $C_{c\bar{c}} \approx 36$, for $\sqrt{s} = 13$ TeV.

Using the information in figure 3 for the coefficients C_{gg} and $C_{b\bar{b}}$ one can compute the diphoton production cross section for different values of the resonance mass. This dependence is shown in the plots of figure 4, for a fixed scale $\Lambda = 4.2$ and 4.8 TeV of the effective operator and different $\tan\beta$ and $c_{1,2,3}$ ⁵. Both production channels $b\bar{b}$ and gg of H, A contribute, see figure 5. In some cases, the cross section can be large, $\sigma \sim$ few fb, well above its value in the MSSM alone and this can conflict with the latest data [4]. To avoid this situation, as seen in figure 4, a larger m_X and/or larger Λ and/or large $\tan\beta$ may be required, correlated as shown. If the value of σ is known from experiments and assuming $X = H, A$, these plots together with constraints on SM-like Higgs physics can be used to set stronger bounds on the correlation of Λ with $\tan\beta$ and $m_{H,A}$. We shall do this shortly for $m_{H,A}$ in the range $0.5 - 1$ TeV.

⁵We keep c_j close to unity (while freely adjusting Λ), otherwise the effective scale of new physics (operator \mathcal{L}_j) is changed to $\Lambda/\sqrt{|c_j|}$.

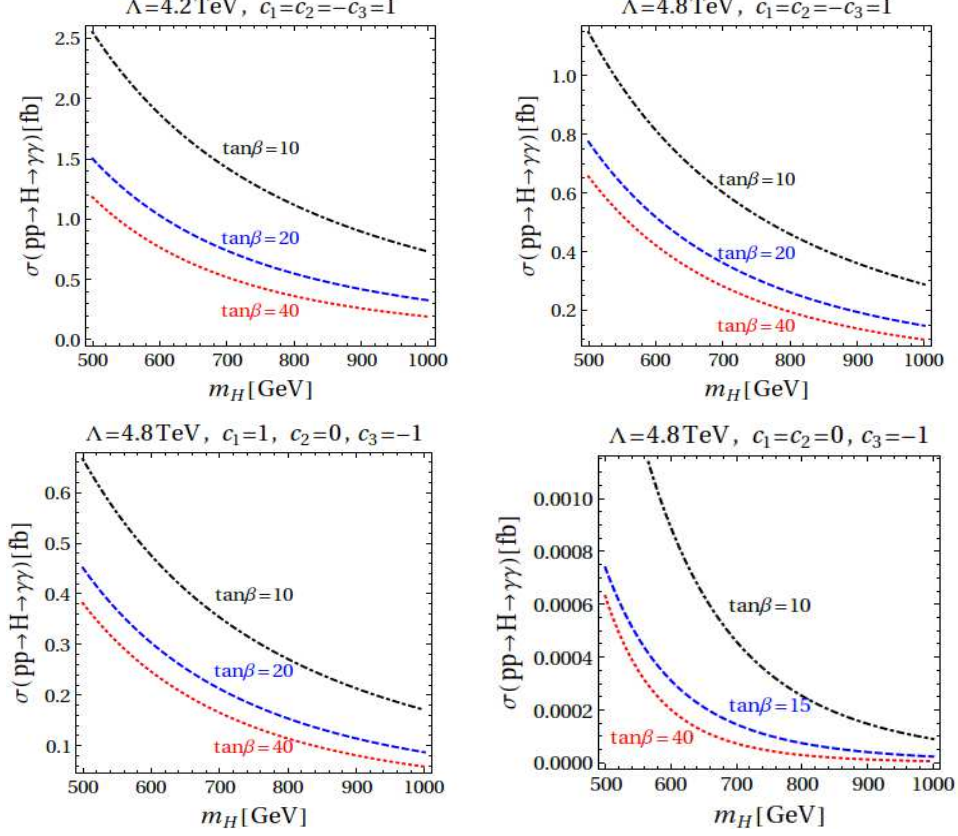


Figure 4: The diphoton production cross section for fixed Λ as a function of the mass m_X ($X = H$) for different $\tan\beta$ and coefficients $c_{1,2,3}$ of the effective operators. Similar dependence (nearly identical) exists for $X = A$. The largest cross section for a given Λ is obtained if all $c_{1,2,3} \neq 0$ and have appropriate relative signs (shown). Of individual contributions for the same effective scale, the largest correction to σ is from \mathcal{L}_3 , then \mathcal{L}_1 .

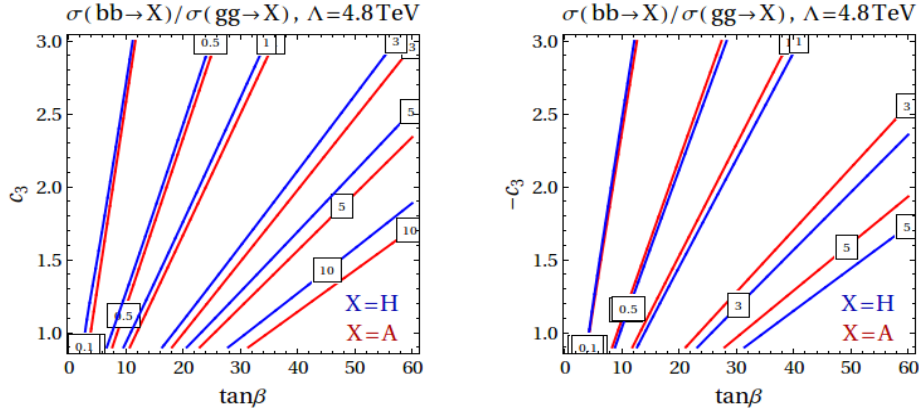


Figure 5: Ratios of production cross sections: $\sigma(b\bar{b} \rightarrow X)/\sigma(gg \rightarrow X)$ for $X = H$ in blue and $X = A$ in red, for $c_3 > 0$ (left plot) and $c_3 < 0$ (right plot). Depending on $\tan\beta$ and $|c_3|$ either gg or $b\bar{b}$ production mechanism may dominate or they have comparable cross sections. Here we chose $m_{H,A} = 750$ GeV, for illustration.

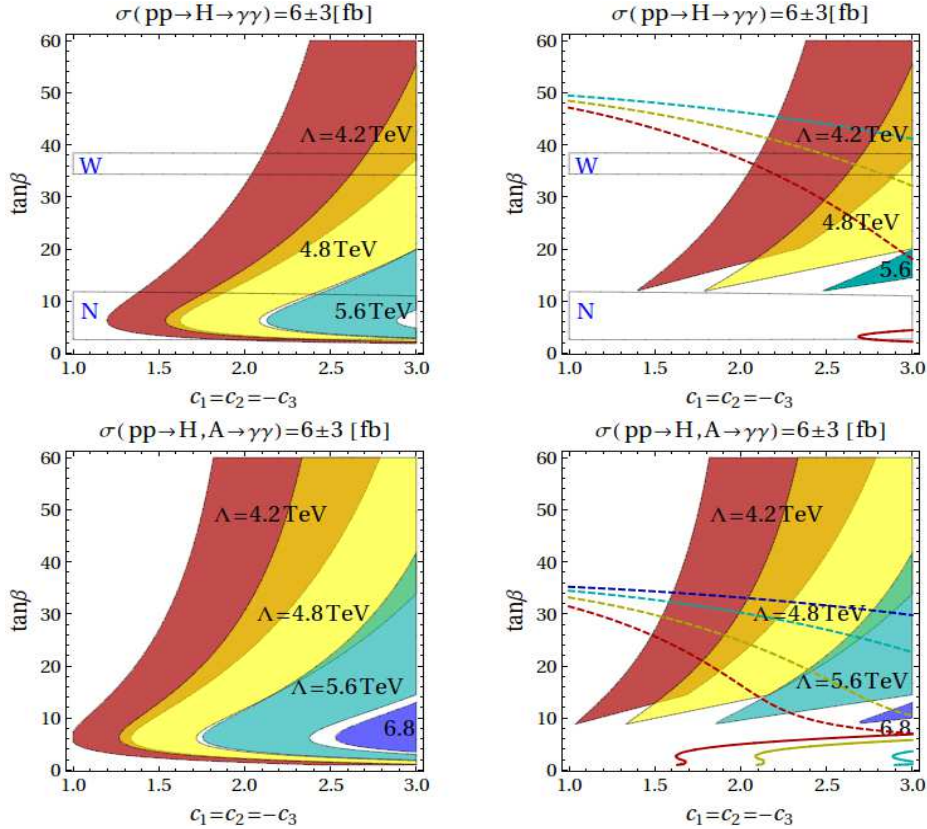


Figure 6: Parameter space for the diphoton cross section σ , mediated by H (top) and by both A, H , mass degenerate, at $m_{H,A} = 750$ GeV (bottom). Nearly identical plots to H exist for A alone. Each coloured area has $\sigma = 6 \pm 3$ fb with a fixed Λ . Areas of overlapping colours (e.g. red and yellow, shown in orange) correspond to two different Λ , ($3 \leq \sigma \leq 9$). Region “N” corresponds to a narrow resonance $\Gamma_{H,A} \leq 5$ GeV; region “W” has a wide width of $40 \leq \Gamma_{H,A} \leq 50$ GeV. For $12 \leq \tan \beta \leq 36$, $\Gamma_{H,A}$ has intermediate values (fig.2). Region “W” is excluded by the constraint $\mathcal{R}_{b\bar{b}} \equiv \Gamma_{X \rightarrow b\bar{b}}/\Gamma_{X \rightarrow \gamma\gamma} \leq 500(r/5)$, $X = A, H$. The plots in the right column have CMS bounds on κ_γ and κ_g applied which excluded the low $\tan \beta$ regions. A dotted (continuous) curve in a colour rules out the area (if present) in the same colour situated above (below) that curve, due to $b\bar{b}$ ($t\bar{t}$) searches, respectively [7]. The corresponding region of this “resonance”, for fixed Λ , is the area in a given colour below the dotted curve *in the same colour*, in the right column of plots.

2.4 The dependence of σ on $m_{H,A}$ and the missing 750 GeV “resonance”

As seen in the previous section, $\mathcal{L}_{1,2,3}$ may provide a diphoton production cross section that is as large as few fb, as initially reported by ATLAS/CMS [1], at $m_X = 750$ GeV, ($X = H, A$), now ruled out by recent additional data [4]. In the following we first detail the exclusion limits on the scale Λ , correlated with $\tan \beta$, from the absence of this resonance. We then consider the general case of varying $0.5 \text{ TeV} \leq m_{H,A} \leq 1 \text{ TeV}$ and explore the dependence of σ on $m_{H,A}$, Λ and $\tan \beta$, under the experimental constraints from the SM-like higgs couplings hgg and $h\gamma\gamma$ and from $b\bar{b}$ and $t\bar{t}$ searches. Both production channels of $X = H, A$ are included and either of these may dominate (figure 5).

Figure 6 shows the parameter space giving the initially found $\sigma(pp \rightarrow H, A \rightarrow \gamma\gamma) =$

6 ± 3 fb at $m_X = 750$ GeV, mediated by H or A or both (mass degenerate case⁶). The allowed parameter space is similar for A and H . In this figure the relative signs of $|c_j| \sim 1$ were chosen to maximise the diphoton production for given Λ . Note that the effective cutoff of an operator is ultimately $\Lambda/\sqrt{|c_j|}$.

Narrow resonance: For low $2 \leq \tan \beta \leq 12$ (figures 2, 6) one has a narrow width, $\Gamma_{H,A} \leq 5$ GeV. For $\tan \beta \leq 8$, the gg production channel of H, A dominates; for $8 \leq \tan \beta \leq 12$ the $b\bar{b}$ channel is also relevant (figure 5).

Let us see the effect of the constraints from the SM-like higgs (h) rates. In figure 6 the low $\tan \beta$ region contributes to $h \rightarrow \gamma\gamma$ (photons) and $h \rightarrow gg$ (gluons) and can even enhance (reduce) the rate of $h \rightarrow \gamma\gamma$ beyond the SM value for negative (positive) $c_{1,2}$, respectively [20]⁷. Define by κ_γ and κ_g the scaling coefficients of the amplitude of the SM-like higgs couplings to $\gamma\gamma$ and gg ; then one has [21] (see also [22, 23]):

$$\begin{aligned} \text{CMS, 68\%CL :} & \quad \kappa_\gamma = 0.965 \pm 0.175, & \quad \kappa_g = 0.835 \pm 0.105 & \quad (15) \\ \text{ATLAS, 68\%CL :} & \quad \kappa_\gamma = 1.2 \pm 0.15, & \quad \kappa_g = 1.04 \pm 0.14 & \quad (16) \end{aligned}$$

We used the CMS constraint in fig. 6 at 95% CL, with $\kappa_j^2 = \Gamma_{h \rightarrow jj} / \Gamma_{h \rightarrow jj}^{SM}$, $j = \gamma, g$. As a result, $2 \leq \tan \beta \leq 10$ or so is in conflict with these constraints from h decays and this region, largely overlapping with our narrow width regime, is ruled out. Further, $t\bar{t}$ searches also rule out some parameter space close to $1 \leq \tan \beta < 8$ but the bound found is in general weaker than the above bounds from h signals⁸. As a result, the parametric region in figure 6 corresponding to this narrow “resonance” is a small region at the tip of each coloured area of fixed Λ with $\tan \beta \approx 10 - 12$.

Broad resonance: The region $34 \leq \tan \beta \leq 38$ ($40 \leq \Gamma_{H,A} \leq 50$ GeV, fig.2) marked as “W” in figs. 6, where the $b\bar{b}$ production mechanism dominates (if $|c_3| \approx 1 - 2$, fig.5), is ruled out by constraints such as those in Table 1, of which $\mathcal{R}_{b\bar{b}} < 500$ is the strongest. Further, $b\bar{b}$ searches with a cross section bound ≤ 5 pb at 13 TeV (Table 1 in [7]) are also marked in figs.6, with a dotted curve in a given colour that rules out any area *in the same colour* situated *above* that curve. This leaves a parametric area bordered by $\tan \beta \leq 25$ with $\Gamma_X \leq 25$ GeV ($\tan \beta \leq 18$, $\Gamma_X \leq 12$ GeV) for $\sigma \approx 3$ fb ($\sigma \approx 9$ fb) respectively, for mass degenerate A and H and $\Lambda/\sqrt{|c_j|}$ fixed.

With this resonance now ruled out, one must then exclude its parametric region bordered by $10 \leq \tan \beta \leq 25$ ($10 \leq \tan \beta \leq 18$) for $\sigma \approx 3$ fb ($\sigma \approx 9$ fb), respectively and demand the effective scale be larger than $\Lambda/\sqrt{|c_j|} \approx 4.2$ TeV. We checked that similar bounds apply for mildly different values of $c_{1,2,3}$ and from unity. These bounds are relevant provided that all $\mathcal{L}_{1,2,3}$ in eq.(3) contribute. Since \mathcal{L}_3 is the dominant contribution, if $c_3 = 0$ then one has a much smaller diphoton cross section. If $c_2 = 0$ (or $c_1 = 0$) and $c_3 \neq 0$ i.e. only $\mathcal{L}_{1,3}$ ($\mathcal{L}_{2,3}$) are present, total σ is again reduced; one may still reach $\sigma \sim 3$ fb by compensating with an increase of the remaining coefficients, but then $\Lambda/\sqrt{|c_j|}$ may become too low for a reliable effective expansion.

⁶In the decoupling limit we use, valid for $m_A = 750$ GeV, the mass splitting δm between A and H can be neglected $m_H^2 = m_A^2 + m_Z^2 \sin^2[2\beta]$, so $\delta m \leq 2$ GeV for $\tan \beta > 3$ and decreases further at larger $\tan \beta$.

⁷This is due to coefficients $\hat{c}_{\gamma\gamma}$ or $c_{\gamma\gamma}$ which contribute at low $\tan \beta$, see eqs.(6), (9) for $\alpha \rightarrow \beta - \pi/2$.

⁸The bound used for $t\bar{t}$ searches is $\sigma(pp \rightarrow X \rightarrow t\bar{t}) < 2250$ fb (13 TeV), see Table 1 in [7].

\mathcal{R}_{ZZ}	$\mathcal{R}_{Z\gamma}$	\mathcal{R}_{WW}	$\mathcal{R}_{t\bar{t}}$	$\mathcal{R}_{b\bar{b}}$	\mathcal{R}_{gg}
$6(r/5)$	$6(r/5)$	$20(r/5)$	$300(r/5)$	$500(r/5)$	$1300(r/5)$

Table 1: Upper bounds on the partial widths $\mathcal{R}_{ab} = \Gamma_{X \rightarrow ab} / \Gamma_{X \rightarrow \gamma\gamma}$, ($X = H, A$), obtained from 8 TeV data scaled to 13 TeV, with $r = \sigma_{13\text{TeV}} / \sigma_{8\text{TeV}} \approx 5$ and a wide resonance $\Gamma_{H,A} = 45$ GeV [7]. They apply at large $\tan\beta$. $\mathcal{R}_{b\bar{b}}$ is the strongest bound.

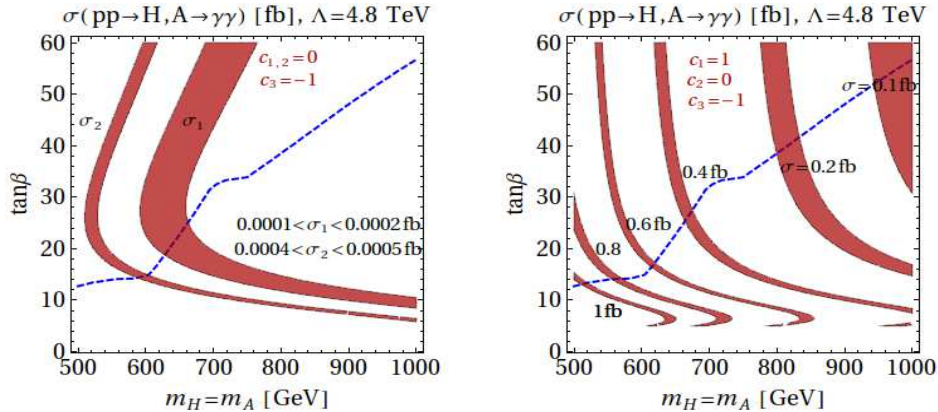


Figure 7: Parameter space for different values of the diphoton cross section σ , mediated by both A, H (mass degenerate) for a varying mass $m_{H,A}$ with $\Lambda = 4.8$ TeV and $c_{1,2} = 0, c_3 = -1$ (left) and $c_1 = -c_3 = 1, c_2 = 0$ (right). The red regions in the left plot have σ in the range shown while in the right plot, their left edge has σ larger by 0.03 fb from the values shown. The partonic integral coefficients dependence on $m_{H,A}$ is included. The CMS bounds on κ_γ and κ_g excluded a small low $\tan\beta < 6$ regions. The dotted curve (in blue) corresponds to a bound from $b\bar{b}$ searches (observed values, see figure 6 in [26]). The $t\bar{t}$ searches bound (observed values, see figure 2 in [27]) is also imposed but for the cases considered here for $c_{1,2,3}$ does not constrain the parameter space. The allowed parametric region is then the area below the dotted curve.

We return now to a general case of varying $m_{H,A}$ in the range $0.5 \text{ TeV} \leq m_{H,A} \leq 1 \text{ TeV}$. Figure 7 shows the dependence of the diphoton cross section σ on $m_{H,A}$ and $\tan\beta$, under the experimental constraints from hgg and $h\gamma\gamma$ couplings and $b\bar{b}, t\bar{t}$ searches. The cross section bounds for the $b\bar{b}$ and $t\bar{t}$ searches depend on $m_{H,A}$; we used the observed values (95% CL) for $b\bar{b}$ searches of figure 6 in [26] and for $t\bar{t}$ searches of figure 2 in [27], for the range of m_X considered in our figure 7. These values were scaled to $\sqrt{s} = 13$ TeV. The dependence of the parton coefficients on $m_{H,A}$ is also included (see figure 3).

Large values of diphoton cross section $\sigma \sim 0.1 - 1$ fb (well above the MSSM value) are obtained when both \mathcal{L}_3 and \mathcal{L}_1 are present, for $\Lambda = 4.8$ TeV (right plot in fig.7). For $|c_3|$ only mildly different from unity $|c_3| \sim 1.3$ or if also $c_2 \neq 0$, then σ increases further from the values shown. Unlike for the 750 GeV “resonance”, there are now regions of low $\tan\beta < 10$ with a large diphoton production such as: $\sigma \sim 1$ fb for $m_{H,A} \sim 550 - 650$ GeV, or $\sigma \sim 0.4$ fb for $m_{H,A} \sim 1$ TeV, that pass all the above constraints⁹. Increasing Λ above ~ 5 TeV or considering instead only individual operators, e.g. dominant \mathcal{L}_3 (left plot in figure 7), can reduce σ significantly. This ends our analysis of the diphoton cross section for $m_{H,A}$ in the range $0.5 - 1$ TeV.

⁹The low $\tan\beta$ region may also be interesting for the naturalness issue, see later.

3 Microscopic models for $\mathcal{L}_{1,2,3}$ and higgs mass corrections

Having seen the role of $\mathcal{L}_{1,2,3}$ on the diphoton cross section, we now explain their possible origin in a renormalizable model. We also address their effect on the higgs sector masses.

3.1 Microscopic origin of effective operator(s) $\mathcal{L}_{1,2,3}$

$\mathcal{L}_{1,2,3}$ may be generated in the MSSM with additional states with mass of order Λ . To see this, consider a massive gauge singlet S that couples to the higgs and gauge sector as in:

$$\delta L = \int d^4\theta S^\dagger S + \left\{ \int d^2\theta \left[\mu H_1 \cdot H_2 + \lambda S H_1 \cdot H_2 + \frac{1}{2} M_1 S^2 + f(S) \text{Tr}(W^\alpha W_\alpha) \right] + \text{h.c.} \right\} \quad (17)$$

$f(S) = S/M_2$ is a gauge kinetic function of a SM subgroup and M_2 some high mass scale. To generate all $\mathcal{L}_{1,2,3}$ the coupling to the gauge sector is extended to $SU(3) \times SU(2)_L \times U(1)_Y$. We integrate out the superfield S via its eqs of motion and find after some algebra and consistent truncation of higher orders

$$\begin{aligned} \delta L = & \int d^4\theta \left[2 \left| \frac{\lambda}{M_1} \right|^2 |H_1 \cdot H_2|^2 \right] \\ & + \int d^2\theta \left[\mu H_1 \cdot H_2 - \frac{\lambda^2}{2M_1} (H_1 \cdot H_2)^2 - \frac{\lambda}{M_1 M_2} (H_1 \cdot H_2) \text{Tr}(W^\alpha W_\alpha) \right] + \text{h.c.} + \mathcal{O}(1/M_1^3) \end{aligned} \quad (18)$$

In the rhs of the above equation there are two more terms: $-1/(2M_1 M_2^2) (\text{Tr} W^2)^2|_F$ and also $2\lambda/(M_1^2 M_2) (H_1 \cdot H_2)^\dagger \text{Tr} W^2|_D$; since we choose $M_2 \geq M_1$, they are sub-leading, $\mathcal{O}(1/M_1^3)$, and can be ignored. The last line in eq.(18) shows our operators of $d = 6$ and $d = 5$ generated simultaneously when integrating S . However eq.(17) does not yet provide a UV complete, renormalizable setup, since it still contains a $d = 5$ effective operator: $(S/M_2) \text{Tr}(W^\alpha W_\alpha)|_F$. One possibility is that this operator is generated if S has additional, renormalizable couplings to massive vector-like states under the SM gauge group, of mass $\mathcal{O}(M_2)$, as shown in diagram (1) of figure 8. Integrating out the vector-like states then generates this remaining operator¹⁰. We thus have a microscopic origin of $\mathcal{L}_{1,2,3}$.

Eq.(18) also contains a $d = 6$ operator $|H_1 \cdot H_2|_D^2$ which brings a negative correction to the SM-like Higgs mass $\delta m_h^2 = -4v^2 |\lambda|^2 \mu^2 / \Lambda^2 + \mathcal{O}(1/\tan^2 \beta)$ [18] (for $M_1 = \Lambda$); this correction is less relevant (being sub-leading to that of eq.(21), see later). Finally, taking $M_1 \sim M_2 \sim \Lambda$ and comparing eq.(18) to (3), we identify $\lambda = c_j/2$ and $c_0 = -\lambda^2/2 = -c_j^2/8$.

Another way to generate $(H_1 \cdot H_2) \text{Tr}(W^\alpha W_\alpha)_F$ is at one-loop, without a massive singlet. One considers only copies of massive vector-like states as in diagram (2) of fig.8.

To conclude, a heavy diphoton resonance ($X = H, A$) of large cross section is present if SM-charged, massive vector-like states (and possibly a singlet) are present beyond MSSM; after decoupling, they generate $\mathcal{L}_{1,2,3}$. Other ways to generate the $d = 6$ operator(s) may exist. The vector-like states have a significant impact on the gauge couplings unification at one-loop, unless they are complete $SU(5)$ multiplets [28].

¹⁰ $(S/M_2) \text{Tr} W^\alpha W_\alpha|_F$ is a moduli-dependent gauge kinetic term, generic in supergravity or string theory.

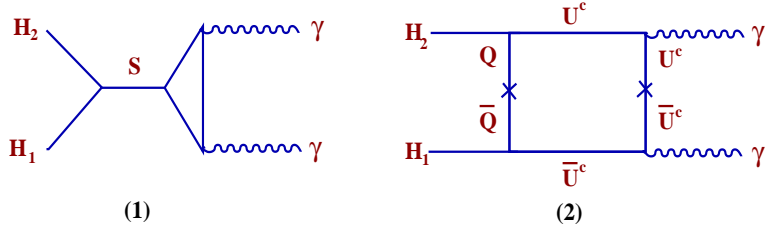


Figure 8: Diagrams generating the $d = 6$ operator $(H_1.H_2) \text{Tr}(W^\alpha W_\alpha)|_F$ at one-loop level. Diagram (1) corresponds to the approach in eqs.(17), (18), with a loop of vector-like states of mass $\propto M_2$ that generate $(S/M_2)\text{Tr}(W^\alpha W_\alpha)|_F$ of eq.(17), while (classical) integration of S generates the needed $d = 6$ operator. Diagram (2) (plus another one as (2) but with $Q \leftrightarrow U^c, \bar{Q} \leftrightarrow \bar{U}^c$) show how to generate the $d = 6$ operator in one stage, without a massive singlet S . A large number of vector-like states can compensate the loop suppression.

3.2 Implications for Higgs sector masses

Unlike the “gluon” operator \mathcal{L}_3 , the “electroweak” operators $\mathcal{L}_{1,2}$ of eq.(3) also impact on the higgs masses $m_{h,H}^2 = M_{h,H}^2 + \Delta m_{h,H}^2$. Here $M_{h,H}$ denote the MSSM value. We find¹¹

$$\Delta m_{h,H}^2 = \frac{8\rho}{\Lambda^2} [g_1^2 c_1 + g_2^2 c_2] + \mathcal{O}\left[\frac{1}{\Lambda^3}\right] \quad (19)$$

where

$$\rho = \frac{v^4}{32} \sin 2\beta \left[1 \pm \frac{1}{4\sqrt{w}} [8m_A^2 - (4 + 3\delta)m_Z^2 + 6\delta m_Z^2 \cos 2\beta + 3(4m_A^2 - \delta m_Z^2) \cos 4\beta] \right] \quad (20)$$

and $w = [(m_A^2 - m_Z^2) \cos 2\beta + \delta m_Z^2 \sin^2 \beta]^2 + \sin^2 2\beta (m_A^2 + m_Z^2)^2$; the upper (lower) signs correspond to h (H) and δ is shown in Appendix B. These corrections bring a modest increase of the SM-like higgs mass $\Delta m_h \sim 1\text{GeV}$ for $c_{1,2} = \mathcal{O}(1)$, with a largest value for small $\tan \beta$, with little dependence on m_A . An even smaller correction is found for m_H . The mass of the CP-odd Higgs boson is also modified, see eq.(B-2). These corrections have little impact on the previous diphoton analysis.

As we saw in the previous sub-section, a leading $d = 5$ operator

$$\mathcal{L}_0 = \frac{c_0}{\Lambda} \int d^2\theta (H_1.H_2)^2 + \text{h.c.} \quad (21)$$

may also be generated from the UV complete (renormalizable) model, without direct contribution to the diphoton cross section. Its correction to the higgs mass is [16, 18]

$$\Delta m_{h,H}^2 = \left[2\mu \frac{c_0}{\Lambda} \right] \rho_1 + \left[2\mu \frac{c_0}{\Lambda} \right]^2 \rho_2 + \mathcal{O}\left[\frac{1}{\Lambda^3}\right] \quad (22)$$

where $\rho_{1,2}$ are shown in eq.(B-4). With $c_0 \mu > 0$, a numerical analysis shows a significant increase of m_h for small $\tan \beta < 10$, by as much as $\approx 10\text{ GeV}$ [16]. This increase can reduce the amount of EW scale fine tuning by a significant factor [16, 24] relative to its MSSM

¹¹using the first ref in [18] and adding a one-loop effect, too (top Yukawa).

value at low $\tan\beta$ region (which is an otherwise very fine tuned MSSM region).

4 Conclusions

Current searches for “new physics” at the LHC bring increasingly strong constraints on the MSSM-like models. Their parameter space becomes smaller, with negative implications for their naturalness. However, simple extensions of their minimal higgs sector, parametrised by effective (supersymmetric) operators, relax the parameter space or even improve naturalness. We studied the constraints on such operators that can enhance dramatically the couplings of the higgs sector to SM gauge bosons and thus the heavy diphoton production.

Minimal models (MSSM) have a small diphoton cross section at large $m_{H,A}$, unless one is fine-tuning the parameters. We identified leading operators of dimension $d=6$ in the higgs sector $\mathcal{L}_j \sim c_j/\Lambda^2 (H_1.H_2)\text{Tr}(W^\alpha W_\alpha)_j|_F$, $j=1,2,3$, $c_j = \mathcal{O}(1)$, that enhance the couplings to SM gauge bosons, with \mathcal{L}_3 having the dominant effects. For $m_{H,A}$ in the range $0.5 \text{ TeV} \leq m_{H,A} \leq 1 \text{ TeV}$, the combination $\mathcal{L}_1 + \mathcal{L}_3$ can lead to a large diphoton production $\sigma \sim 0.1 - 1 \text{ fb}$, well above the MSSM value. The analysis included both gg and $b\bar{b}$ production mechanisms (of $X=H,A$) and either of these may dominate. We examined the correlation between the diphoton cross section σ and the values of m_X , Λ and $\tan\beta$, under the experimental constraints from SM-like higgs couplings hgg and $h\gamma\gamma$ (due to mixing) and from $b\bar{b}$ and $t\bar{t}$ searches. These give $\Lambda/\sqrt{|c_j|} > 4.8 \text{ TeV}$ where the effective approach can still be trusted, for $m_{H,A}$ between $0.5 - 1 \text{ TeV}$.

Regarding the initially claimed resonance at $m_X=750 \text{ GeV}$ with even larger σ (few fb), this could be reached if all $\mathcal{L}_{1,2,3}$ contribute. Recent data ruled out this resonance, then not all $\mathcal{L}_{1,2,3}$ are simultaneously present or the scale $\Lambda/\sqrt{|c_j|}$ is larger than $4 - 5 \text{ TeV}$.

We showed how to generate the $d=6$ effective operator(s) from a UV complete (renormalizable) theory. This is possible by integrating out additional massive SM vector-like states beyond the MSSM spectrum, and eventually a massive singlet too, of mass $\mathcal{O}(\Lambda)$. An additional $d=5$ operator in the higgs sector may also be generated at the same time, that does not affect directly the diphoton production, but may improve naturalness.

Appendix:

A Loop functions and couplings

In this section we present the expressions of the coefficients a_{\dots}^{loop} , b_{\dots}^{loop} , c_{\dots}^{loop} , used in the text (section 2.1). To compute them and to fix the notation, we need the couplings of MSSM fields h, H, A to fermions and gauge bosons. These are, in a standard notation

$$\begin{aligned}
-\Delta\mathcal{L} = & k_t \frac{m_t}{v} h \bar{t} t + k_b \frac{m_b}{v} h \bar{b} b + \frac{2m_W^2}{v} (k_w h + \tilde{k}_w H) W^{+\mu} W_\mu^- \\
& + \tilde{k}_t \frac{m_t}{v} H \bar{t} t + \tilde{k}_b \frac{m_b}{v} H \bar{b} b + i\bar{k}_t \frac{m_t}{v} A \bar{t} \gamma^5 t + i\bar{k}_b \frac{m_b}{v} A \bar{b} \gamma^5 b
\end{aligned} \quad (\text{A-1})$$

where

$$\begin{aligned}
k_t &= \frac{\cos \alpha}{\sin \beta}, & k_b &= -\frac{\sin \alpha}{\cos \beta}, & k_w &= \sin(\beta - \alpha) \\
\tilde{k}_t &= \frac{\sin \alpha}{\sin \beta}, & \tilde{k}_b &= \frac{\cos \alpha}{\cos \beta}, & \tilde{k}_w &= \cos(\beta - \alpha), \\
\bar{k}_t &= \cot \beta, & \bar{k}_b &= -\tan \beta.
\end{aligned} \quad (\text{A-2})$$

Here α is the mixing angle in the Higgs sector. In this paper we work in the decoupling limit (m_A large). Then $\alpha \rightarrow \beta - \pi/2$ and $k_{t,b,w} = 1$ while $\tilde{k}_t = -\cot \beta$, $\tilde{k}_b = \tan \beta$, $\tilde{k}_w = 0$. Then we find the coefficients of the effective operators in eqs.(9), (10), as follows [25]

$$\begin{aligned}
a_{gg}^{loop} &= \bar{k}_t \bar{A}_g^{(t)} + \bar{k}_b \bar{A}_g^{(b)} \approx (0.0771 + 0.7064i) \cot \beta - (0.00281 + 0.00194i) \tan \beta \\
a_{\gamma\gamma}^{loop} &= \bar{k}_w \bar{A}_\gamma^{(W)} + \bar{k}_t \bar{A}_\gamma^{(t)} + \bar{k}_b \bar{A}_\gamma^{(b)} \approx (0.13702 + 1.256i) \cot \beta + (0.00125 - 0.00086i) \tan \beta \\
a_{\gamma z}^{loop} &= a_{zz}^{loop} = a_{ww}^{loop} = 0.
\end{aligned}$$

and

$$\begin{aligned}
b_{gg}^{loop} &= \tilde{k}_t \tilde{A}_g^{(t)} + \tilde{k}_b \tilde{A}_g^{(b)} \approx -(0.441 + 1.112i) \cot \beta + (-0.00538 + 0.00387i) \tan \beta \\
b_{\gamma\gamma}^{loop} &= \tilde{k}_w \tilde{A}_\gamma^{(W)} + \tilde{k}_t \tilde{A}_\gamma^{(t)} + \tilde{k}_b \tilde{A}_\gamma^{(b)} \approx -(0.783 + 1.98i) \cot \beta + (-0.00239 + 0.00172i) \tan \beta \\
b_{\gamma z}^{loop} &= \tilde{k}_t \tilde{A}_{\gamma z}^{(t)} + \tilde{k}_b \tilde{A}_{\gamma z}^{(b)} \approx (0.12513 + 0.32821i) \cot \beta + (0.00103 - 0.000043i) \tan \beta \\
b_{ww}^{loop} &= b_{zz}^{loop} = 0.
\end{aligned} \quad (\text{A-3})$$

and finally

$$c_{gg}^{loop} = k_t A_g^{(t)} + k_b A_g^{(b)} \approx 0.970 + 0.0894i \quad (\text{A-4})$$

$$c_{\gamma\gamma}^{loop} = k_w A_\gamma^{(W)} + k_t A_\gamma^{(t)} + k_b A_\gamma^{(b)} \approx -6.51 + 0.0397i \quad (\text{A-5})$$

where coefficients $A_{\dots}^{(i)}$ are one-loop form factors, presented below.

For h one has the following form factors

$$A_g^{(\xi)} = \frac{3}{4}A_{1/2}(\tau_\xi), \quad \xi = t, b. \quad (\text{A-6})$$

$$A_\gamma^{(\xi)} = N_c Q_\xi^2 A_{1/2}(\tau_\xi), \quad \xi = t, b. \quad (\text{A-7})$$

$$A_\gamma^{(W)} = A_1(\tau_W) \quad (\text{A-8})$$

$$A_{Z\gamma}^{(W)} = \cos \theta_w A_1(\tau_W, \lambda_W) \quad (\text{A-9})$$

$$A_{Z\gamma}^{(t)} = \frac{N_c Q_t}{\cos^2 \theta_w} \frac{(2T_3^{(t)} - 4Q_t \sin^2 \theta_w)}{\cos \theta_w} A_{1/2}(\tau_t, \lambda_t) \quad (\text{A-10})$$

and for H

$$\tilde{A}_g^{(\xi)} = \frac{3}{4}A_{1/2}(\tilde{\tau}_\xi), \quad \xi = t, b. \quad (\text{A-11})$$

$$\tilde{A}_\gamma^{(\xi)} = N_c Q_\xi^2 A_{1/2}(\tilde{\tau}_\xi), \quad \xi = t, b. \quad (\text{A-12})$$

$$\tilde{A}_{\gamma_z}^{(\xi)} = \frac{N_c Q_\xi}{\cos \theta_w} (2T_3^{(\xi)} - 4Q_\xi \sin^2 \theta_w) A_{1/2}(\tilde{\tau}_\xi, \lambda_\xi), \quad \xi = t, b. \quad (\text{A-13})$$

and for A :

$$\bar{A}_g^{(\xi)} = \frac{3}{4}\bar{A}_{1/2}(\bar{\tau}_\xi), \quad \xi = t, b. \quad (\text{A-14})$$

$$\bar{A}_\gamma^{(\xi)} = N_c Q_\xi^2 \bar{A}_{1/2}(\bar{\tau}_\xi), \quad \xi = t, b. \quad (\text{A-15})$$

where $\tau_i = 4m_i^2/m_h^2$, $\tilde{\tau}_i = 4m_i^2/m_H^2$, $\bar{\tau}_i = 4m_i^2/m_A^2$, $N_c = 3$, $Q_t = 2/3$, and $Q_b = -1/3$. $T_3^{(t)} = 1/2$, $T_3^{(b)} = -1/2$ and $\lambda_\xi = 4m_\xi^2/m_Z^2$. Finally

$$\begin{aligned} A_{1/2}(\tau) &= 2\tau^2 [\tau^{-1} + (\tau^{-1} - 1)f(\tau^{-1})] , \\ \bar{A}_{1/2}(\tau) &= \tau f(\tau^{-1}), \\ A_1(\tau) &= -\tau^2 [2\tau^{-2} + 3\tau^{-1} + 3(2\tau^{-1} - 1)f(\tau^{-1})] , \\ A_{1/2}(\tau, \lambda) &= I_1(\tau, \lambda) - I_2(\tau, \lambda) , \end{aligned} \quad (\text{A-16})$$

where

$$\begin{aligned} I_1(\tau, \lambda) &= \frac{\tau\lambda}{2(\tau - \lambda)} + \frac{\tau^2\lambda^2}{2(\tau - \lambda)^2} [f(\tau^{-1}) - f(\lambda^{-1})] + \frac{\tau^2\lambda}{(\tau - \lambda)^2} [g(\tau^{-1}) - g(\lambda^{-1})] , \\ I_2(\tau, \lambda) &= -\frac{\tau\lambda}{2(\tau - \lambda)} [f(\tau^{-1}) - f(\lambda^{-1})] , \end{aligned} \quad (\text{A-17})$$

and

$$f(x) = \begin{cases} \arcsin^2 \sqrt{x} & x \leq 1 \\ -\frac{1}{4} \left[\log \frac{1 + \sqrt{1 - x^{-1}}}{1 - \sqrt{1 - x^{-1}}} - i\pi \right]^2 & x > 1 , \end{cases} \quad (\text{A-18})$$

$$g(x) = \begin{cases} \sqrt{x^{-1}-1} \arcsin \sqrt{x} & x \leq 1 \\ \frac{\sqrt{1-x^{-1}}}{2} \left[\log \frac{1+\sqrt{1-x^{-1}}}{1-\sqrt{1-x^{-1}}} - i\pi \right]^2 & x > 1. \end{cases} \quad (\text{A-19})$$

B Mass corrections

The MSSM higgses masses are, at one-loop for dominant top Yukawa (upper sign for h)

$$M_{h,H}^2 = \frac{1}{2} \left\{ m_A^2 + m_Z^2 + \delta m_Z^2 \sin^2 \beta \mp \sqrt{w} \right\} \quad (\text{B-1})$$

The mass of CP-odd Higgs is also modified by the effective operators

$$m_A^2 = \frac{2B\mu}{\sin 2\beta} - \frac{2v^2}{\sin 2\beta} \left[\frac{c_0}{\Lambda} \mu \right] - \frac{v^4 \cos^2 2\beta}{4 \sin 2\beta} \left[\frac{g_1^2 c_1}{\Lambda^2} + \frac{g_2^2 c_2}{\Lambda^2} \right] + \mathcal{O}\left(\frac{1}{\Lambda^3}\right) \quad (\text{B-2})$$

and $w = [(m_A^2 - m_Z^2) \cos 2\beta + \delta m_Z^2 \sin^2 \beta]^2 + \sin^2 2\beta (m_A^2 + m_Z^2)^2$. Here δ is the top/stop correction to the Higgs potential, as in $\Delta V_h = (1/8) (g_1^2 + g_2^2) \delta |h_u|^4$ where

$$\begin{aligned} \delta &\equiv \frac{3h_t^4}{g^2 \pi^2} \left[\ln \frac{M_{\tilde{t}}}{m_t} + \frac{X_t}{4} + \frac{1}{32\pi^2} (3h_t^2 - 16g_3^2) \left(X_t + 2 \ln \frac{M_{\tilde{t}}}{m_t} \right) \ln \frac{M_{\tilde{t}}}{m_t} \right] \\ X_t &\equiv \frac{2(A_t - \mu \cot \beta)^2}{M_{\tilde{t}}^2} \left(1 - \frac{(A_t - \mu \cot \beta)^2}{12 M_{\tilde{t}}^2} \right). \end{aligned} \quad (\text{B-3})$$

with $M_{\tilde{t}}^2 \equiv m_{\tilde{t}_1} m_{\tilde{t}_2}$, and g_3 is the QCD coupling.

The values of $\rho_{1,2}$ in eq.(22) are

$$\rho_1 = v^2 \sin 2\beta \left\{ 1 \pm \frac{(m_A^2 + m_Z^2)}{\sqrt{w}} \right\} \quad (\text{B-4})$$

$$\rho_2 = \frac{v^4}{4\mu^2} \sin^2 2\beta \pm \frac{v^4}{\sqrt{w}} \left\{ -1 + \frac{1}{2\mu^2} (m_A^2 + m_Z^2) \sin^2 2\beta \right\} \pm \frac{1}{w^{3/2}} (m_A^2 + m_Z^2)^2 v^4 \sin^2 2\beta$$

with the upper (lower) sign for h (H).

Acknowledgements: The work of D.M.G. was supported by a grant of the Romanian National Authority for Scientific Research (CNCS-UEFISCDI) under project number PN-II-ID-PCE-2011-3-0607. The work of H.M.L. was supported in part by Basic Science Research Program through the National Research Foundation of Korea (NRF) funded by the Ministry of Education, Science and Technology (NRF-2016R1A2B4008759).

References

- [1] LHC seminar “ATLAS and CMS physics results from Run 2” talks by Jim Olsen and Marumi Kado, CERN 15 Dec 2015, <https://indico.cern.ch/event/442432/>; ATLAS-CONF-2015-081 “Search for resonances decaying to photon pairs in 3.2 fb⁻¹ of pp collisions at $\sqrt{s} = 13$ TeV with the ATLAS detector” CMS PAS EXO-15-004, “Search for new physics in high mass diphoton events in proton-proton collisions at $\sqrt{s} = 13$ TeV”. The ATLAS collaboration, “Search for resonances in diphoton events with the ATLAS detector at $\sqrt{s} = 13$ TeV,” ATLAS-CONF-2016-018. CMS Collaboration, ‘Search for new physics in high mass diphoton events in 3.3 fb⁻¹ of proton-proton collisions at $\sqrt{s} = 13$ TeV and combined interpretation of searches at 8 TeV and 13 TeV,” CMS-PAS-EXO-16-018.
- [2] G. Aad *et al.* [ATLAS Collaboration], “Search for high-mass diphoton resonances in *pp* collisions at $\sqrt{s} = 8$ TeV with the ATLAS detector,” Phys. Rev. D **92** (2015) 3, 032004 [arXiv:1504.05511 [hep-ex]];
- [3] CMS Collaboration, CMS-PAS-EXO-12-045, “Search for High-Mass Diphoton Resonances in pp Collisions $\sqrt{s} = 8$ TeV with the CMS Detector”.
- [4] CMS Collaboration, CMS-PAS-EXO-16-027, “Search for resonant production of high mass photon pairs using 12.9 fb⁻¹ of proton-proton collisions at $\sqrt{s} = 13$ TeV and combined interpretation of searches at 8 and 13 TeV.” ATLAS Collaboration, ATLAS-CONF-2016-059, “Search for scalar diphoton resonances with 15.4 fb⁻¹ of data collected at $\sqrt{s}=13$ TeV in 2015 and 2016 with the ATLAS detector”.
- [5] C. Beskidt, W. de Boer, D. I. Kazakov and S. Wayand, “Higgs Branching Ratios in Minimal and Next-to-Minimal Supersymmetry Scenarios Surveyed,” arXiv:1602.08707 [hep-ph]. R. S. Gupta, S. Jger, Y. Kats, G. Perez and E. Stamou, “Interpreting a 750 GeV Diphoton Resonance,” arXiv:1512.05332 [hep-ph].
- [6] A. Strumia, “Interpreting the 750 GeV digamma excess: a review,” arXiv:1605.09401 [hep-ph].
- [7] R. Franceschini *et al.*, “What is the $\gamma\gamma$ resonance at 750 GeV?,” JHEP **1603** (2016) 144 [arXiv:1512.04933 [hep-ph]].
- [8] For early works, see: A. Falkowski, O. Slone, T. Volansky, “Phenomenology of a 750 GeV Singlet,” arXiv:1512.05777 [hep-ph]. J. Ellis, S. A. R. Ellis, J. Quevillon, V. Sanz and T. You, “On the Interpretation of a Possible ~ 750 GeV Particle Decaying into $\gamma\gamma$,” JHEP **1603** (2016) 176 [arXiv:1512.05327 [hep-ph]]. T. Robens and T. Stefaniak, “LHC Benchmark Scenarios for the Real Higgs Singlet Extension of the Standard Model,” arXiv:1601.07880 [hep-ph]. M. J. Dolan, J. L. Hewett, M. Kramer and T. G. Rizzo, “Simplified Models for Higgs Physics: Singlet Scalar and Vector-like Quark Phenomenology,” arXiv:1601.07208 [hep-ph]. J. Ellis, S. A. R. Ellis, J. Quevillon, V. Sanz and T. You, “On the Interpretation of a Possible ~ 750 GeV Particle Decaying into $\gamma\gamma$,” JHEP **1603** (2016) 176 [arXiv:1512.05327 [hep-ph]]. For a full list of references see [6].
- [9] W. Altmannshofer, J. Galloway, S. Gori, A. L. Kagan, A. Martin and J. Zupan, “On the 750 GeV di-photon excess,” arXiv:1512.07616 [hep-ph]. L. Berthier, J. M. Cline, W. Shepherd and M. Trott, “Effective interpretations of a diphoton excess,” arXiv:1512.06799 [hep-ph]. S. Di Chiara, L. Marzola and M. Raidal, “First interpretation of the 750 GeV di-photon resonance at the LHC,” arXiv:1512.04939 [hep-ph].
- [10] J. F. Kamenik, B. R. Safdi, Y. Soreq and J. Zupan, “Comments on the diphoton excess: critical reappraisal of effective field theory interpretations,” JHEP **1607** (2016) 042 [arXiv:1603.06566 [hep-ph]].

- [11] A. Djouadi and A. Pilaftsis, “The 750 GeV Diphoton Resonance in the MSSM,” arXiv:1605.01040 [hep-ph]. A. Bharucha, A. Djouadi and A. Goudelis, “Threshold enhancement of diphoton resonances,” arXiv:1603.04464 [hep-ph]. D. Choudhury and K. Ghosh, “The LHC Diphoton excess at 750 GeV in the framework of the Constrained Minimal Supersymmetric Standard Model,” arXiv:1605.00013 [hep-ph].
- [12] S. V. Demidov and D. S. Gorbunov, “On sgoldstino interpretation of the diphoton excess,” arXiv:1512.05723 [hep-ph]. C. Petersson and R. Torre, “The 750 GeV diphoton excess from the goldstino superpartner,” arXiv:1512.05333 [hep-ph]. J. A. Casas, J. R. Espinosa and J. M. Moreno, “The 750 GeV Diphoton Excess as a First Light on Supersymmetry Breaking,” arXiv:1512.07895 [hep-ph]. R. Ding, Y. Fan, L. Huang, C. Li, T. Li, S. Raza and B. Zhu, “Systematic Study of Diphoton Resonance at 750 GeV from Sgoldstino,” arXiv:1602.00977 [hep-ph]. B. Bellazzini, R. Franceschini, F. Sala and J. Serra, “Goldstones in Diphotons,” JHEP **1604** (2016) 072 [arXiv:1512.05330 [hep-ph]].
- [13] Y. L. Tang and S. h. Zhu, “NMSSM extended with vector-like particles and the diphoton excess on the LHC,” arXiv:1512.08323 [hep-ph]. F. Wang, W. Wang, L. Wu, J. M. Yang and M. Zhang, “Interpreting 750 GeV Diphoton Resonance in the NMSSM with Vector-like Particles,” arXiv:1512.08434 [hep-ph]. M. Badziak, M. Olechowski, S. Pokorski and K. Sakurai, “Interpreting 750 GeV Diphoton Excess in Plain NMSSM,” arXiv:1603.02203 [hep-ph]. F. Staub *et al.*, “Precision tools and models to narrow in on the 750 GeV diphoton resonance,” arXiv:1602.05581 [hep-ph].
- [14] U. Ellwanger and C. Hugonie, “A 750 GeV Diphoton Signal from a Very Light Pseudoscalar in the NMSSM,” JHEP **1605** (2016) 114 [arXiv:1602.03344 [hep-ph]].
- [15] R. Ding, L. Huang, T. Li and B. Zhu, “Interpreting 750 GeV Diphoton Excess with R-parity Violation Supersymmetry,” arXiv:1512.06560 [hep-ph]. F. Domingo, S. Heinemeyer, J. S. Kim and K. Rolbiecki, “The NMSSM lives - with the 750 GeV diphoton excess,” arXiv:1602.07691 [hep-ph]. B. C. Allanach, P. S. B. Dev, S. A. Renner and K. Sakurai, “Di-photon Excess Explained by a Resonant Sneutrino in R-parity Violating Supersymmetry,” arXiv:1512.07645 [hep-ph].
- [16] S. Cassel, D. M. Ghilencea and G. G. Ross, “Fine tuning as an indication of physics beyond the MSSM,” Nucl. Phys. B **825** (2010) 203 [arXiv:0903.1115 [hep-ph]].
- [17] D. Piriz and J. Wudka, “Effective operators in supersymmetry,” Phys. Rev. D **56** (1997) 4170 [hep-ph/9707314].
- [18] I. Antoniadis, E. Dudas, D. M. Ghilencea and P. Tziveloglou, “MSSM Higgs with dimension-six operators,” Nucl. Phys. B **831** (2010) 133 [arXiv:0910.1100 [hep-ph]]. M. Carena, K. Kong, E. Ponton and J. Zurita, “Supersymmetric Higgs Bosons and Beyond,” Phys. Rev. D **81** (2010) 015001 [arXiv:0909.5434 [hep-ph]]. I. Antoniadis, E. Dudas, D. M. Ghilencea and P. Tziveloglou, “Beyond the MSSM Higgs with d=6 effective operators,” Nucl. Phys. B **848** (2011) 1 [arXiv:1012.5310 [hep-ph]].
- [19] H. L. Lai *et al.* [CTEQ Collaboration], “Global QCD analysis of parton structure of the nucleon: CTEQ5 parton distributions,” Eur. Phys. J. C **12** (2000) 375 [hep-ph/9903282]. S. Kretzer, H. L. Lai, F. I. Olness and W. K. Tung, “Cteq6 parton distributions with heavy quark mass effects,” Phys. Rev. D **69** (2004) 114005 [hep-ph/0307022].
- [20] M. Berg, I. Buchberger, D. M. Ghilencea and C. Petersson, “Higgs diphoton rate enhancement from supersymmetric physics beyond the MSSM,” Phys. Rev. D **88** (2013) 2, 025017 [arXiv:1212.5009 [hep-ph]].

- [21] The Review of Particle Physics (2015) K.A. Olive et al. (Particle Data Group), Chin. Phys. C, **38**, 090001 (2014), <http://pdg.lbl.gov/>
- [22] C. D. Froggatt, C. R. Das, L. V. Laperashvili and H. B. Nielsen, “Diphoton decay of the Higgs boson and new bound states of top and antitop quarks,” Int. J. Mod. Phys. A **30** (2015) no.21, 1550132 [arXiv:1501.00139 [hep-ph]].
- [23] J. Ellis and T. You, “Updated Global Analysis of Higgs Couplings,” JHEP **1306** (2013) 103 [arXiv:1303.3879 [hep-ph]].
- [24] S. Cassel and D. M. Ghilencea, “A Review of naturalness and dark matter prediction for the Higgs mass in MSSM and beyond,” Mod. Phys. Lett. A **27** (2012) 1230003 [arXiv:1103.4793 [hep-ph]].
- [25] M. Carena, I. Low and C. E. M. Wagner, “Implications of a Modified Higgs to Diphoton Decay Width,” JHEP **1208** (2012) 060 doi:10.1007/JHEP08(2012)060 [arXiv:1206.1082 [hep-ph]]. I. Low, J. Lykken and G. Shaughnessy, “Have We Observed the Higgs (Imposter)?,” Phys. Rev. D **86** (2012) 093012 doi:10.1103/PhysRevD.86.093012 [arXiv:1207.1093 [hep-ph]].
- [26] V. Khachatryan *et al.* [CMS Collaboration], “Search for neutral MSSM Higgs bosons decaying into a pair of bottom quarks,” JHEP **1511** (2015) 071 doi:10.1007/JHEP11(2015)071 [arXiv:1506.08329 [hep-ex]].
- [27] S. Chatrchyan *et al.* [CMS Collaboration], “Searches for new physics using the $t\bar{t}$ invariant mass distribution in pp collisions at $\sqrt{s}=8\text{TeV}$,” Phys. Rev. Lett. **111** (2013) no.21, 211804 Erratum: [Phys. Rev. Lett. **112** (2014) no.11, 119903] doi:10.1103/PhysRevLett.111.211804, 10.1103/PhysRevLett.112.119903 [arXiv:1309.2030 [hep-ex]].
- [28] D. Ghilencea, M. Lanzagorta and G. G. Ross, “Unification predictions,” Nucl. Phys. B **511** (1998) 3 [hep-ph/9707401]. G. Amelino-Camelia, D. Ghilencea and G. G. Ross, “The Effect of Yukawa couplings on unification predictions and the nonperturbative limit,” Nucl. Phys. B **528** (1998) 35 [hep-ph/9804437].